JOURNAL OF THERMOPHYSICS AND HEAT TRANSFER
Vol. 26, No. 3, July–September 2012

Stagnation-Point Flow and Heat Transfer of a Viscous, Compressible Fluid on a Cylinder

Hamid Mohammadiun* and Asghar B. Rahimi†
Ferdowsi University of Mashhad, Mashhad, Iran

DOI: 10.2514/1.T3833

The steady-state, viscous, compressible flow and heat transfer in the vicinity of an axisymmetric stagnation point of an infinite stationary cylinder with constant wall temperature are investigated. The impinging freestream is steady and with a constant strain rate $\bar{k}$. Exact solutions of the Navier–Stokes equations and energy equation are derived in this problem. A reduction of these equations is obtained by use of appropriate transformations introduced for the first time. The general self-similar solution is obtained when the wall temperature of the cylinder is constant. All of the aforementioned solutions are presented for Reynolds numbers $Re = \bar{k}a^2/2\nu$ ranging from 0.01 to 1000, selected values of compressibility factor, and different values of Prandtl numbers where a is cylinder radius and ν is kinematic viscosity of the fluid. For all Reynolds numbers and surface temperatures, as the compressibility factor increases, both components of the velocity field, heat-transfer coefficient, and shear stresses increase, whereas the pressure function decreases.

Nomenclature

a	=	cylinder radius
$c(\eta)$	=	density ratio
$f(\eta)$	=	function
$h(z)$	=	local heat-transfer coefficient
k	=	thermal conductivity
$\bar{k}$	=	freestream strain rate
P	=	nondimensional pressure
p	=	fluid pressure
Pr	=	Prandtl number
q_w	=	heat flow at wall
r, z	=	cylindrical coordinates
Re	=	Reynolds number
T	=	temperature
T_w	=	wall temperature
T_∞	=	freestream temperature

Greek

β	=	compressibility factor
$\Gamma(\eta)$	=	function related to density
η	=	similarity variable
$\theta(\eta)$	=	nondimensional temperature
μ	=	viscosity
ν	=	kinematic viscosity
$\rho(\eta)$	=	fluid density
ρ_∞	=	freestream density
σ	=	shear stress

I. Introduction

EXISTING solutions of the problem of axisymmetric stagnation-point flow and heat transfer on either a cylinder or a flat plate are for viscous, incompressible fluid. These studies started by Hiemenz [1], who obtained an exact solution of the Navier–Stokes equations governing the two-dimensional stagnation-point flow on a flat plate, and were continued by Homann [2] with an analogous axisymmetric study and by Howarth [3] and Davey [4], whose results for stagnation flow against a flat plate for asymmetric cases were presented. Wang [5,6] was the first to find an exact solution for the problem of axisymmetric stagnation flow on an infinite stationary circular cylinder; this was continued by Gorla's works [7–11], which are a series of steady and unsteady flows and heat transfer over a circular cylinder in the vicinity of the stagnation point for the cases of constant axial movement and the special case of axial harmonic motion of a nonrotating cylinder. Cunning et al. [12] have considered the stagnation flow problem on a rotating circular cylinder with constant angular velocity; Grosch and Salwen [13] as well as Takhar et al. [14] studied special cases of unsteady viscous flow on an infinite circular cylinder. The most recent works of the same types are the ones by Saleh and Rahimi [15] and Rahimi and Saleh [16,17], which are exact solution studies of a stagnation-point flow and heat transfer on a circular cylinder with time-dependent axial and rotational movements, as well as studies by Abbasi and Rahimi [18–21], which are exact solutions of stagnation-point flow and heat transfer but on a flat plate. Some existing compressible flow studies but in the stagnation region of bodies and by using boundary layer equations include the study by Subhashini and Nath [22] as well as Kumari and Nath [23,24], which are in the stagnation region of a body, and work of Katz [25] as well as Afzal and Ahmad [26], Libby [27], and Gersten et al. [28], which are all general studies in the stagnation region of a body.

The problem of stagnation-point flow and heat transfer for the case of compressible fluid has not been considered so far. In this research work, solution of the problem of axisymmetric stagnation-point flow and heat transfer is presented for the case of compressible, viscous fluid on a stationary cylinder with constant wall temperature. An exact solution of the Navier–Stokes equations and the energy equation is obtained. The self-similar solution is reached by introducing for the first time similarity variables. Sample distributions of shear stress and temperature fields at Reynolds numbers ranging from 0.01 to 1000 are presented for different values of Prandtl numbers and fluid compressibility factor.

II. Problem Formulation

Flow is considered in cylindrical coordinates (r, φ, z) with corresponding velocity components (u, v, w); see Fig. 1. We consider the laminar steady compressible flow and heat transfer of a viscous fluid in the neighborhood of an axisymmetric stagnation point of a stationary infinite circular cylinder with constant wall

Received 2 October 2011; revision received 31 December 2011; accepted for publication 3 January 2012.

*Ph.D. Student, P.O. Box 91775-1111.

†Professor, Faculty of Engineering, P.O. Box 91775-1111; rahimiab@yahoo.com (Corresponding Author).

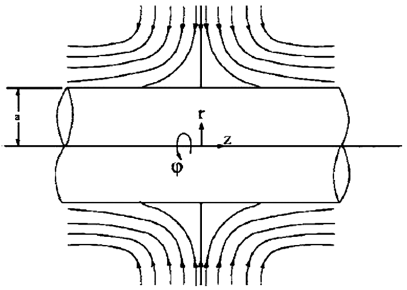

Fig. 1 Schematic diagram of a stationary cylinder.

temperature. An external axisymmetric radial stagnation flow of strain rate $\bar{k}$ impinges on the cylinder of radius a, centered at $r = 0$. The steady Navier–Stokes and energy equations in cylindrical polar coordinates governing the axisymmetric compressible flow and heat transfer are as follows.

Mass,

$$\frac{\partial(\rho u)}{\partial r} + \frac{\rho u}{r} + \frac{\partial(\rho w)}{\partial z} = 0 \tag{1}$$

r momentum,

$$u\frac{\partial(\rho u)}{\partial r} + w\frac{\partial(\rho u)}{\partial z} = -\frac{\partial P}{\partial r} + \nu\left\{\frac{1}{r}\frac{\partial}{\partial r}\left[r\frac{\partial(\rho u)}{\partial r}\right] - \frac{(\rho u)}{r^2} + \frac{\partial^2(\rho u)}{\partial z^2}\right\} \tag{2}$$

z momentum,

$$u\frac{\partial(\rho w)}{\partial r} + w\frac{\partial(\rho w)}{\partial z} = -\frac{\partial P}{\partial z} + \nu\left\{\frac{1}{r}\frac{\partial}{\partial r}\left[r\frac{\partial(\rho w)}{\partial r}\right] + \frac{\partial^2(\rho w)}{\partial z^2}\right\} \tag{3}$$

and energy,

$$\rho u\frac{\partial T}{\partial r} + \rho w\frac{\partial T}{\partial z} = \frac{\mu}{Pr}\frac{1}{r}\frac{\partial}{\partial r}\left(r\frac{\partial T}{\partial r}\right) \tag{4}$$

where p, ρ, ν, and T are the fluid pressure, density, kinematic viscosity, and temperature inside the boundary layer and after the impingement has occurred, respectively. The boundary conditions for the velocity field are

$$r = a: \qquad u = 0, \qquad w = 0 \tag{5}$$

$$r \to \infty: \qquad u = -\bar{k}(r - a^2/r), \qquad w = 2\bar{k}z \tag{6}$$

in which Eq. (5) represents no-slip conditions on the cylinder wall, and the relations of Eq. (6) show that the viscous flow solution approaches, in a manner analogous to the Hiemenz flow, the potential flow solution as $r \to \infty$. This can be confirmed by starting from continuity equation as the following: $-\frac{1}{r}\frac{\partial}{\partial r}(ru) = \frac{\partial w}{\partial z} = \text{constant} = 2\bar{k}$ and integrating in r and z directions with boundary conditions $w = 0$ when $z = 0$ and $u = 0$ when $r = a$.

For the temperature field, we have

$$r = a: \qquad T = T_w = \text{constant} \qquad r \to \infty: \qquad T \to T_\infty \tag{7}$$

where k is the thermal conductivity of the fluid and T_w is temperature at the wall cylinder, respectively, and T_∞ is the freestream temperature.

A reduction of the Navier–Stokes equations is obtained by the following coordinate separation of the velocity field, which are actually modeled by the form of their limits as represented by Eq. (6). Also, a density ratio is introduced to indicate the change of density normal to the surface, which gives back the similarity parameters for the case of an incompressible fluid:

$$u = -\frac{\bar{k}a^2}{r}\frac{\rho_\infty}{\rho(\eta)}f(\eta), \qquad w = \frac{\rho_\infty}{\rho(\eta)}[2\bar{k}cf'(\eta)z]$$
$$p = \rho_\infty \bar{k}^2 a^2 P \tag{8}$$

where

$$\eta = \frac{2}{a^2}\int_a^r \frac{\rho r}{\rho_\infty}\,\mathrm{d}r \tag{9}$$

is a dimensionless radial variable, prime denotes differentiation with respect to η, and ρ_∞ is freestream density. Note that, for the case of incompressible flow ($\rho(\eta) = \text{constant}$), this variable is similar to the one in Wang [5], except that it changes from zero to infinity instead of one to infinity. Transformations (8) satisfy Eq. (1) automatically, and their insertion into Eqs. (2) and (3) yields a coupled system of differential equations in terms of$f(\eta)$, and an expression for the pressure:

$$\Gamma[c^3 f''' + 3c^2 c' f'' + c^2 c'' f' + (c')^2 c f'] + c^2 f'' + cc' f' + Re[1 + c' f f' + c f f'' - c(f')^2] = 0 \tag{10}$$

$$p - p_0 = \int_0^\eta \left[\frac{1}{2}\left(\frac{f}{\Gamma c}\right)^2 - \frac{ff'}{\Gamma c^2} - \frac{1}{Re}(cf')'\right]\mathrm{d}\eta - 2\left(\frac{z}{a}\right)^2 \tag{11}$$

In these equations,

$$c(\eta) = \frac{\rho(\eta)}{\rho_\infty}, \qquad \Gamma(\eta) = 1 + \int_0^\eta \frac{\mathrm{d}\eta}{c(\eta)} \tag{12}$$

and $Re = \frac{\bar{k}a^2}{2\nu}$ is the Reynolds number, and prime indicates differentiation with respect to η. From conditions (5) and (6), the boundary conditions for Eqs. (10) and (11) are as follows:

$$\eta = 0: \qquad f = 0, \qquad f' = 0, \qquad \eta \to \infty: \qquad f' = 1 \tag{13}$$

To model the variation of density with respect to temperature, the following Boussinesq approximation is used assuming low Mach number flow:

$$\rho \approx \rho_\infty[1 - \beta(T - T_\infty)] \Rightarrow \rho/\rho_\infty = c\,(\eta) = 1 - \beta(T - T_\infty) \tag{14}$$

in which β is compressibility factor.

To transform the energy equation into a nondimensional form, we introduce

$$\theta(\eta) = \frac{T(\eta) - T_\infty}{T_w - T_\infty} \tag{15}$$

Making use of Eqs. (8) and (15), the energy equation, with neglecting the small dissipation terms, may be written as

$$\frac{1}{Re.Pr}[\Gamma(c^2\theta'' + cc'\theta') + c\theta'] + f\theta' = 0 \tag{16}$$

with boundary conditions as

$$\eta = 0: \ \theta = 1 \qquad \eta \to \infty: \ \theta = 0 \tag{17}$$

The local heat-transfer coefficient is given by

$$h(z) = \frac{q_w}{T_w - T_\infty} = -\frac{2k}{a}\theta'(0)c(0) \tag{18}$$

Equation (11) for a stationary cylinder is automatically satisfied and, because of $c(\eta)$, Eqs. (10–12) and (16) are dependent. Note that, for the case of incompressible fluid, $\rho(\eta) = \rho_\infty$ and $c(\eta) = 1$, Eq. (10) is exactly reduced to the equation obtained in [5] for the radial component of velocity, and Eq. (16) reduces to the energy equation obtained in [7] with consideration of starting value for the variable η.

Equations (10) and (16), along with boundary conditions (13) and (17), have been solved by using the fourth-order Runge–Kutta method of integration along with a shooting method by Press et al. [29]. Using this method, the initial values were guessed and the integration was repeated until convergence was obtained. In these computations, the grid size was chosen as 0.001, and the truncation error was set to 1×10^{-9}. The equations are descretized using finite difference and are solved using a tridiagonal matrix algorithm.

III. Shear Stress

The shear stress on the surface of the cylinder is obtained from

$$\sigma = \mu\left[\frac{\partial w}{\partial r}\right]_{r=a} \tag{19}$$

where μ is the viscosity of the fluid. Using definition (8), the shear stress at the cylinder surface for self-similar solutions becomes

$$\sigma = \mu[2Kf''(0)z]\frac{2}{a}C(0) \Rightarrow \frac{\sigma a}{4\mu Kz} = f''(0)C(0) \tag{20}$$

Results for $\sigma a/4\mu Kz$ for different values of Reynolds numbers with Prandtl number held constant and for different values of Prandtl numbers with Reynolds number held constant are presented later.

IV. Presentation of Results

In this section, the solution of the self-similar Eqs. (10) and (16), along with surface shear stresses for prescribed values of surface temperature for selected values of Reynolds and Prandtl numbers, are presented.

Sample profiles of the $f(\eta)$ function against η for compressibility factor, $\beta = 0.0033$, $Pr = 0.7$, constant wall temperature $T_w = 300^{ok}$, and for selected values of Reynolds numbers are presented in Fig. 2. As Reynolds number increases, the depth of diffusion of the fluid velocity field in radial direction increases. Effects of variation of compressibility factor on $f(\eta)$ function against η for $T_w = 500^{ok}$, $Pr = 1.0$ and selected value of Reynolds number $Re = 1$ are shown in Fig. 3. For $\beta = 0$, incompressible fluid, the results of Gorla [7] are extracted; it is interesting to note that, as β increases, the depth of diffusion of the fluid velocity field in radial direction increases. Thus,

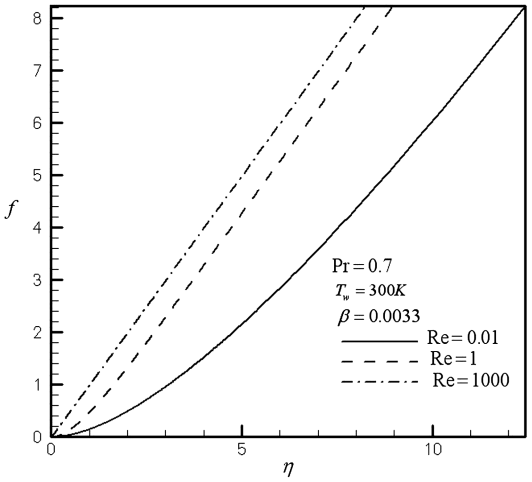

Fig. 2 Variation of f in terms of η at $T_w = 300$ K, $\beta = 0.0033$, and $Pr = 0.7$ for different values of Reynolds numbers.

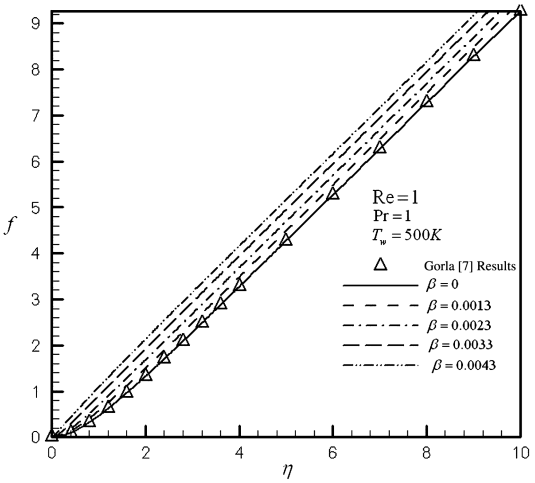

Fig. 3 Variation of f in terms of η at $T_w = 500$ K, $Pr = 1.0$, and $Re = 1.0$ for different values of compressibility factor.

for all the Reynolds numbers, the incompressible fluid case produces the lowest value of radial velocity, and, as compressibility increases, this quantity increases accordingly. It can be shown that the trend of the aforementioned variations are the same for $Re = 10$ and 100. Effect of surface temperature of the cylinder on the depth of the diffusion of the fluid velocity field in radial direction has been depicted in Fig. 4 for $\beta = 0.0033$, $Pr = 0.7$, and selected values of Reynolds numbers. Note that, as the surface temperature of the cylinder increases, this quantity increases for all values of Reynolds numbers. This is expected because the increase of surface temperature and compressibility of the fluid have parallel effects. It can be shown that the trend of the aforementioned variations are the same for $Re = 10$ and 100.

Sample profiles of the $f'(\eta)$ function against η for compressibility factor, $\beta = 0.0033$, $Pr = 0.7$, constant wall temperature $T_w = 300^{ok}$, and for selected values of Reynolds numbers are shown in Fig. 5. Again, as Reynolds number increases, the depth of diffusion of the fluid velocity field in z direction increases. Effects of variations of compressibility factor on $f'(\eta)$ function against η for $T_w = 500^{ok}$, $Pr = 1.0$ and selected value of Reynolds number $Re = 1$ are shown in Fig. 6. For$\beta = 0$, incompressible fluid, the result of Gorla [7] is extracted; it is interesting to note that, as β increases, the depth of the diffusion of the fluid velocity field in the z direction also increases. Again, the incompressible fluid case produces the lowest value of velocity in the z direction, and, as the compressibility factor increases, this quantity increases accordingly. Effect of surface temperature of the cylinder on the depth of the diffusion of the fluid

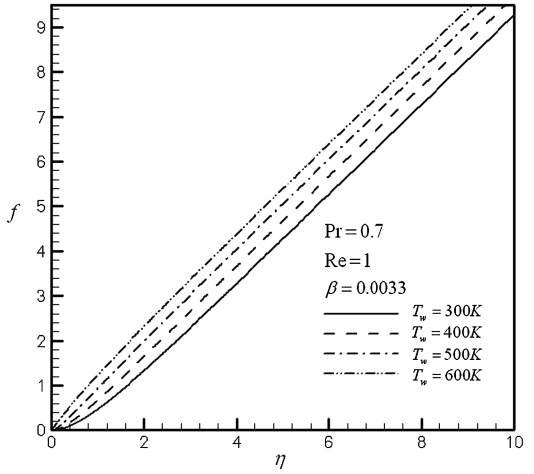

Fig. 4 Variation of f in terms of η at $\beta = 0.0033$, $Pr = 0.7$, and $Re = 1.0$ for different values of surface temperature.

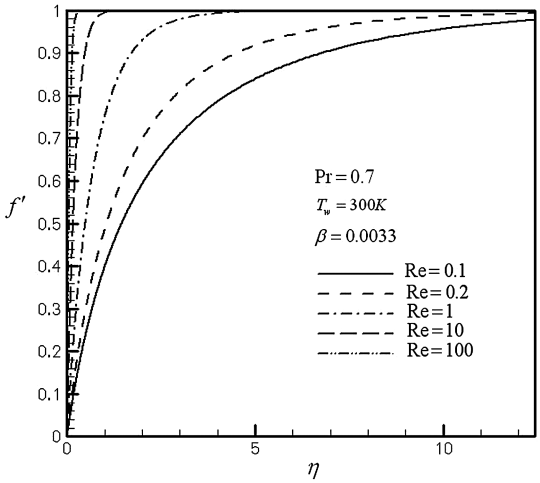

Fig. 5 Variation of f' in terms of η at $\beta = 0.0033$, $Pr = 0.7$, and $T_w = 300^{ok}$ for different values of Reynolds numbers.

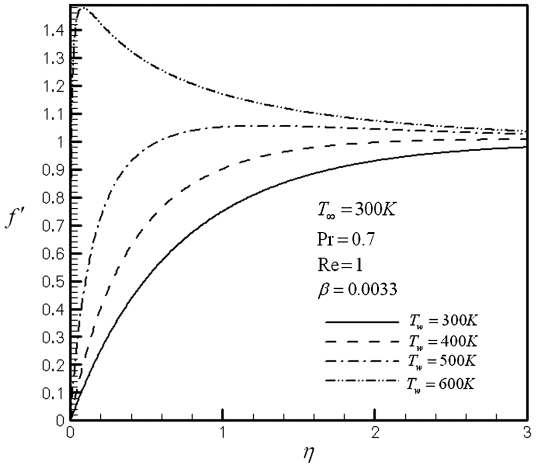

Fig. 8 Variation of f' in terms of η at $Pr = 0.7$, $T_\infty = 300^{ok}$, and $Re = 1.0$ for different values of wall temperature.

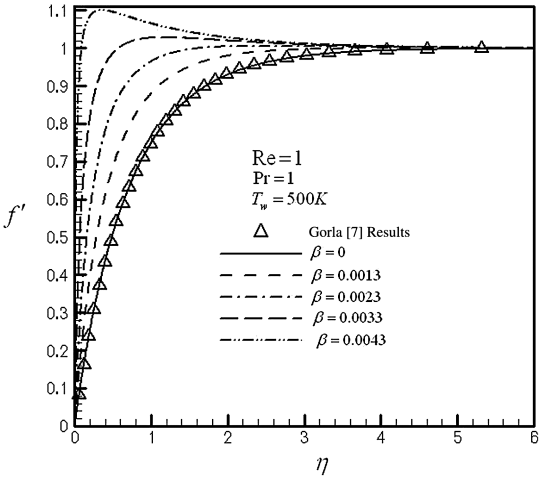

Fig. 6 Variation of f' in terms of η at $Pr = 1.0$, $T_w = 500^{ok}$, and $Re = 1.0$ for different values of compressibility factor.

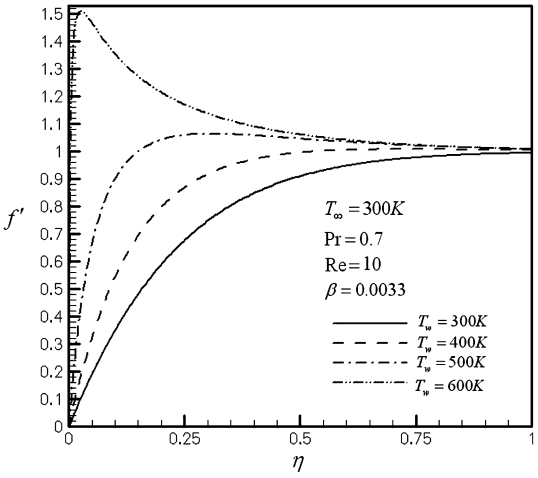

Fig. 9 Variation of f' in terms of η at $Pr = 0.7$, $T_\infty = 300^{ok}$, and $Re = 10.0$ for different values of wall temperature.

velocity field in the z direction has been presented in Figs. 7–9 for $\beta = 0.0033$, $Pr = 0.7$, and selected values of Reynolds numbers. Again as the surface temperature of the cylinder increases, this quantity increases for all values of Reynolds numbers and proves that the effect of surface temperature and compressibility of the fluid are in parallel for the velocity field.

Sample profiles of the $\theta(\eta)$ function against η for the case of constant surface temperature for compressibility factor$\beta = 0.0033$, $Pr = 0.7$, $T_w = 500^{ok}$, and for selected values of Reynolds numbers are depicted in Fig. 10. As Reynolds number increases, the depth of diffusion of the thermal boundary layer decreases, and, in fact, as of

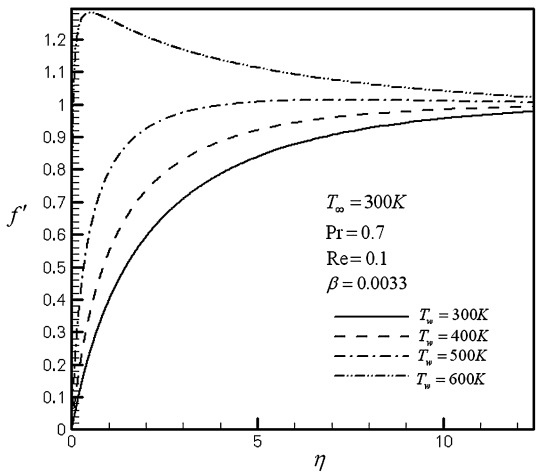

Fig. 7 Variation of f' in terms of η at $Pr = 0.7$, $T_\infty = 300^{ok}$, and $Re = 0.1$ for different values of wall temperature.

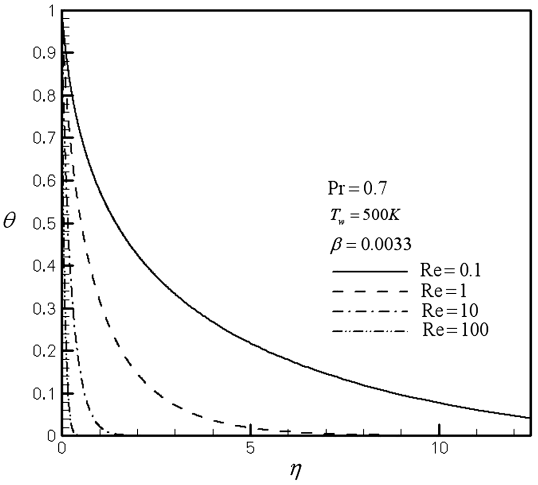

Fig. 10 Variation of θ in terms of η at $Pr = 0.7$, $T_w = 500^{ok}$, and $\beta = 0.0033$ for different values of Reynolds numbers.

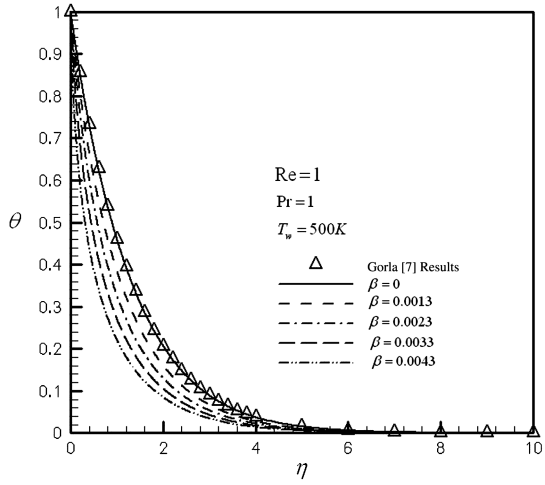

Fig. 11 Variation of θ in terms of η at $Pr = 1.0$, $T_w = 500^{ok}$, and $Re = 1.0$ for different values of compressibility factor.

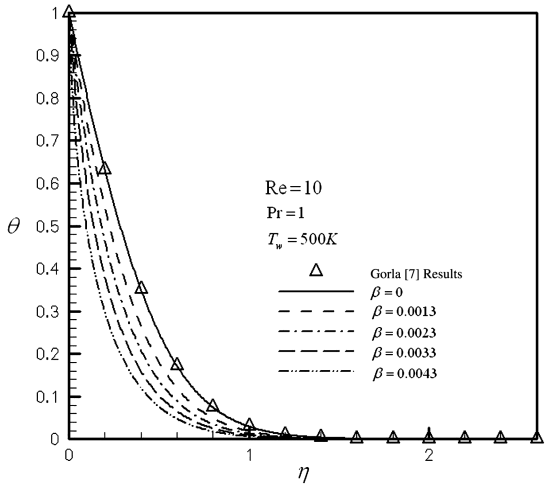

Fig. 12 Variation of θ in terms of η at $Pr = 1.0$, $T_w = 500^{ok}$, and $Re = 1.0$ for different values of compressibility factor.

Eq. (18), the coefficient of heat transfer increases. Effect of variations of compressibility factor on $\theta(\eta)$ function against η for$T_w = 500^{ok}$, $Pr = 1.0$ and selected values of Reynolds numbers are presented in Figs. 11–13. For $\beta = 0$, incompressible fluid, the result of Gorla [7] is

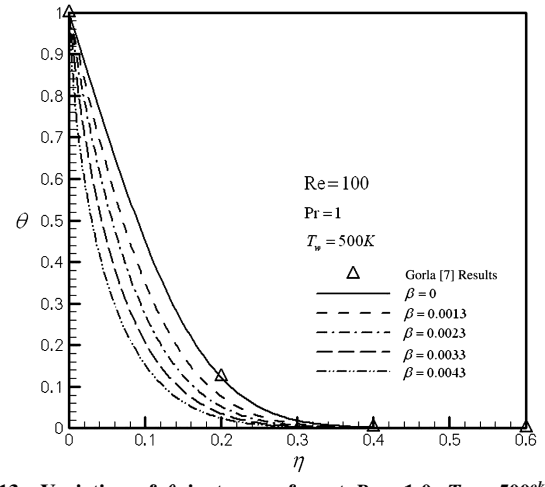

Fig. 13 Variation of θ in terms of η at $Pr = 1.0$, $T_w = 500^{ok}$, and $Re = 100.0$ for different values of compressibility factor.

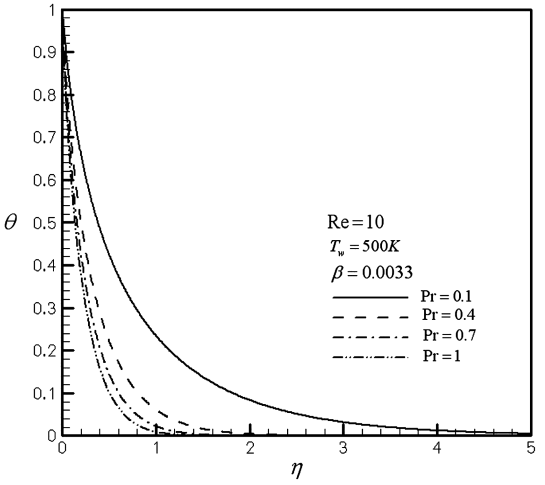

Fig. 14 Variation of θ in terms of η at $T_w = 500^{ok}$, $Re = 10.0$, and $\beta = 0.0033$ for different values of Prandtl numbers.

extracted; it is interesting to note that, as β increases, the depth of the diffusion of the thermal boundary layer decreases. Again, the incompressible fluid case produces the lowest value of heat-transfer coefficient, and, as compressibility increases, this quantity increases accordingly. Effect of variation of constant Prandtl number on $\theta(\eta)$ function for the case of constant surface temperature for compressibility factor $\beta = 0.0033$, $Re = 10$, and $T_w = 500^{ok}$ is shown in Fig. 14. As Prandtl number increases, the depth of diffusion of the thermal boundary layer decreases, and therefore the heat-transfer coefficient increases.

Sample profiles of pressure function against η for the case of $Pr = 0.7$, $T_w = 500^{ok}$, $\beta = 0.0033$, and for selected values of Reynolds numbers are shown in Fig. 15. As expected, by increase of Reynolds number the depth of diffusion of fluid pressure increases. Figure 16 represents pressure for the case of $Pr = 0.7$, $Re = 10$, $\beta = 0.0033$, and different values of cylinder wall temperature. As the wall temperature increases, pressure decreases. Effect of compressibility factor for the case of $Pr = 0.7$, $Re = 1$, and $T_w = 500^{ok}$ is presented in Fig. 17. The largest amount of pressure is produced for the case of incompressible fluid. Effect of increase of Prandtl number on pressure function is depicted in Fig. 18 for the case of $T_w = 500^{ok}$, $Re = 10$, $\beta = 0.0033$. As Prandtl number increases, the pressure function increases as well.

Sample profiles of surface shear stress against cylinder wall temperature are shown in Fig. 19, for the case of $Pr = 0.7$, $\beta = 0.0033$ and for selected values of Reynolds numbers. As expected,

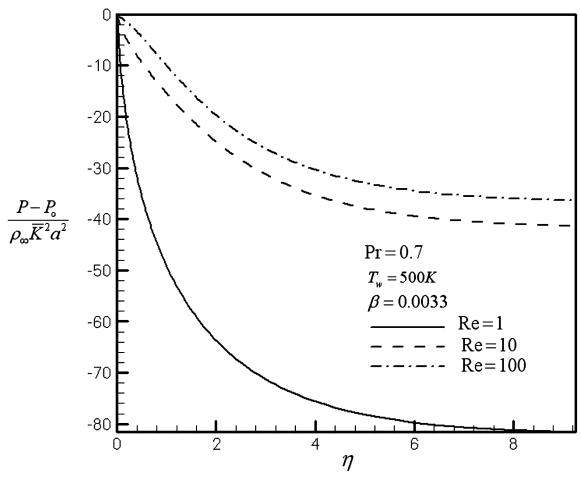

Fig. 15 Variation of pressure function in terms of η at $Pr = 0.7$, $T_w = 500^{ok}$, and $\beta = 0.0033$ for different values of Reynolds numbers.

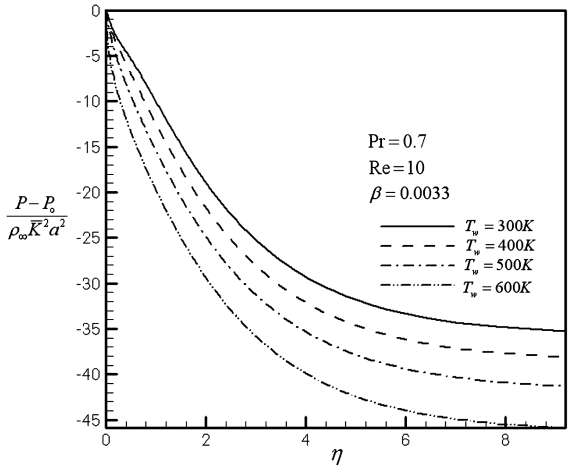

Fig. 16 Variation of pressure function in terms of η at $Pr = 0.7$, $\beta = 0.0033$, and $Re = 10.0$ for different values of wall temperatures.

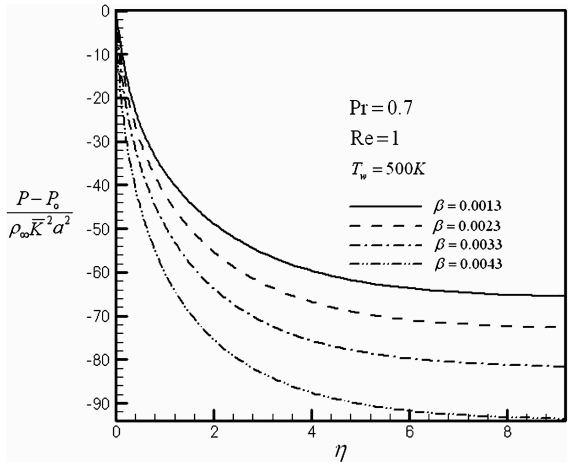

Fig. 17 Variation of pressure function in terms of η at $Pr = 0.7$, $Re = 1.0$, and $T_w = 500^{ok}$ for different values of compressibility factor.

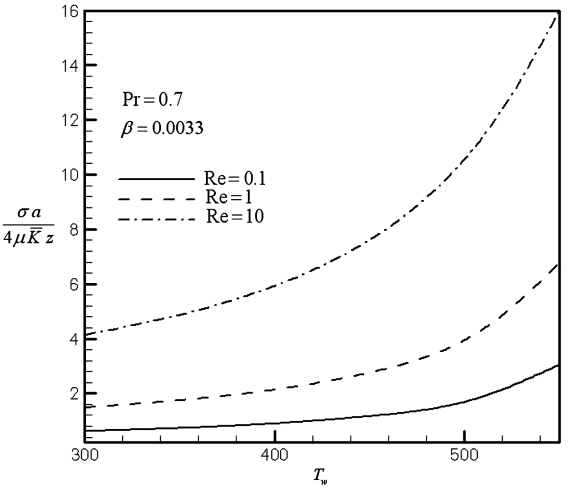

Fig. 19 Variation of shear stress in terms of T_w at $\beta = 0.0033$ and $Pr = 0.7$ for different values of Reynolds numbers.

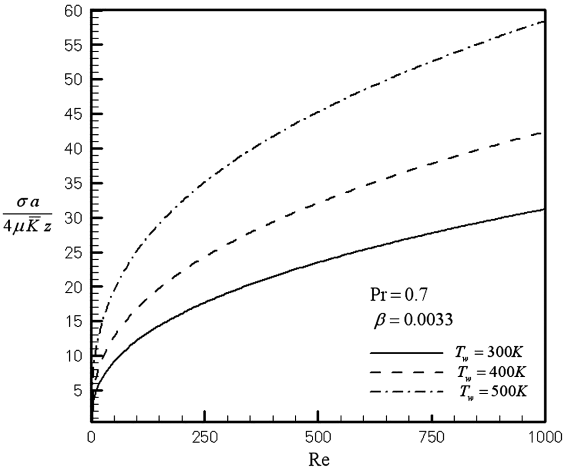

Fig. 20 Variation of shear stress in terms of Re at $\beta = 0.0033$ and $Pr = 0.7$ for different values of wall temperatures.

the higher the Reynolds number, the higher the surface shear stress, and, for individual Reynolds number case, the value of surface shear stress increases with surface temperature. The same information above can be concluded from Fig. 20. Effect of compressibility factor on shear stress against Reynolds number is shown in Fig. 21, for the case of $Pr = 0.7$, $T_w = 500^{ok}$. It is interesting to note that the incompressible fluid case produces the least amount of shear stress.

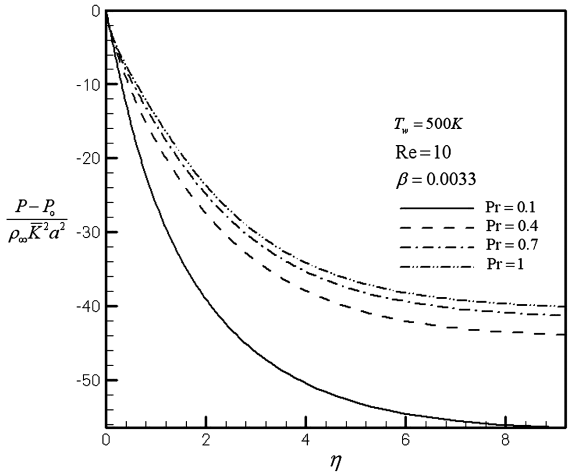

Fig. 18 Variation of pressure function in terms of η at $T_w = 500^{ok}$, $\beta = 0.0033$, and $Re = 10.0$ for different values of Prandtl numbers.

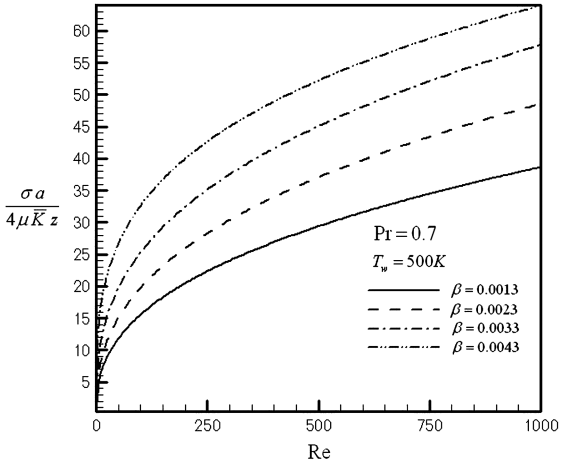

Fig. 21 Variation of shear stress in terms of Re at $T_w = 500^{ok}$ and $Pr = 0.7$ for different values of compressibility factor.

V. Conclusions

An exact solution of the Navier–Stokes equations and energy equation has been obtained for the problem of stagnation-point flow on a stationary circular cylinder with constant wall temperature. A reduction of these equations is obtained by use of appropriate transformations introduced for the first time. The general self-similar solution is obtained when the wall temperature of the cylinder is constant. All of the aforementioned solutions have been presented for Reynolds numbers $Re = \bar{k}a^2/2\nu$ ranging from 0.01 to 1000 and for different values of Prandtl numbers and compressibility factor. For all Reynolds numbers and cylinder wall temperatures, as compressibility factor increases, both components of the velocity field, heat-transfer coefficient, and shear stresses increase, and pressure function decreases. For the case of incompressible fluid, $\rho(\eta) = \rho_\infty$ or $c(\eta) = 1$, and similarity variables and radial component of velocity by Wang [5], as well as energy equation by Gorla [7], are obtained.

Appendix

Details of derivation of Eqs. (10), (11), and (16) are presented next.

$$\begin{aligned}\eta &= \frac{2}{a^2}\int_a^r \frac{\rho r}{\rho_\infty}\,\mathrm{d}r \Rightarrow \frac{\mathrm{d}\eta}{\mathrm{d}r} = \frac{2\rho r}{a^2\rho_\infty} \to \frac{\mathrm{d}\eta}{\mathrm{d}r}\\ &= \frac{2r}{a^2}c(\eta) \to 2r\,\mathrm{d}r = a^2\frac{\mathrm{d}\eta}{c(\eta)} \xrightarrow{\int} \int_a^r 2r\,\mathrm{d}r\\ &= a^2\int_0^\eta \frac{\mathrm{d}\eta}{c(\eta)} \to r^2 - a^2 = a^2\int_0^\eta \frac{\mathrm{d}\eta}{c(\eta)} \to r^2\\ &= a^2\left[1 + \int_0^\eta \frac{\mathrm{d}\eta}{c(\eta)}\right]\end{aligned}$$

With the definition $\Gamma(\eta) = [1 + \int_0^\eta \frac{\mathrm{d}\eta}{c(\eta)}]$, we have $r^2 = a^2\Gamma(\eta)$. To derive pressure, by use of nondimensional pressure as

$$p = \frac{P}{\rho_\infty K^2 a^2} \Rightarrow P = \rho_\infty K^2 a^2 p$$

Start from r momentum

$$\begin{aligned}&u\frac{\partial(\rho u)}{\partial r} + w\frac{\partial(\rho u)}{\partial z}\\ &\quad= -\frac{\partial P}{\partial r} + \nu\left\{\frac{1}{r}\frac{\partial}{\partial r}\left[r\frac{\partial(\rho u)}{\partial r}\right] - \frac{(\rho u)}{r^2} + \frac{\partial^2(\rho u)}{\partial z^2}\right\}\end{aligned}$$

But

$$\begin{aligned}\rho u &= -\frac{Ka^2}{r}\rho_\infty f(\eta) \Rightarrow \frac{\partial(\rho u)}{\partial r} = \frac{Ka^2}{r^2}\rho_\infty f - 2K\rho_\infty c f'\\ &\Rightarrow r\frac{\partial(\rho u)}{\partial r} = \frac{Ka^2}{r}\rho_\infty f - 2K\rho_\infty c f' r\\ &\Rightarrow \frac{\partial}{\partial r}\left[r\frac{\partial(\rho u)}{\partial r}\right] = -\frac{Ka^2}{r^2}\rho_\infty f + \underline{\frac{Ka^2}{r}\rho_\infty f'(\eta)\frac{2r}{a^2}c}\\ &\quad - 2K\rho_\infty (cf')'\frac{2r^2}{a^2}c\underline{-2K\rho_\infty c f'}\\ &\Rightarrow \frac{1}{r}\frac{\partial}{\partial r}\left[r\frac{\partial(\rho u)}{\partial r}\right] = -\frac{Ka^2}{r^3}\rho_\infty f - \frac{4Kr}{a^2}\rho_\infty c(cf')'\end{aligned}$$

Then r momentum is

$$\begin{aligned}&-\frac{Ka^2}{r}\frac{\rho_\infty}{\rho}f(\eta)\left[\frac{Ka^2}{r^2}\rho_\infty f(\eta) - 2K\rho_\infty c f'\right] = -\rho_\infty K^2 a^2\frac{\partial p}{\partial \eta}\frac{2r}{a^2}c\\ &\quad + \nu\left[\underline{-\frac{Ka^2}{r^3}\rho_\infty f} - \frac{4Kr}{a^2}\rho_\infty c(cf')' + \underline{\frac{Ka^2}{r^3}\rho_\infty f}\right]\end{aligned}$$

After omitting underlined phrases,

$$\begin{aligned}&-\frac{K^2a^4}{r^3}\frac{\rho_\infty}{\rho}\rho_\infty f^2 + \frac{2K^2a^2}{r}\frac{\rho_\infty}{\rho}\rho_\infty f f'\\ &\quad= -2\rho_\infty K^2 c r\frac{\partial p}{\partial \eta} - \frac{4K\nu}{a^2}rc\rho_\infty (cf')'\end{aligned}$$

Dividing by $2K^2 r\rho_\infty$ and using $r^2 = a^2\Gamma(\eta)$,

$$\begin{aligned}&-\frac{1}{2}\frac{a^4}{r^4}\frac{f^2}{c} + \frac{a^2}{r^2}\frac{ff'}{c} = -c\frac{\partial p}{\partial \eta} - \frac{2\nu}{Ka^2}c(cf')' \overset{r^2 = a^2\phi(\eta)}{\to} \frac{\partial p}{\partial \eta}\\ &\quad= \frac{1}{2}\left(\frac{f}{\Gamma c}\right)^2 - \frac{ff'}{\Gamma c^2} - \frac{1}{Re}(cf')'\end{aligned}$$

Integrating this, we have

$$p - p_0 = \int_0^\eta \left[\frac{1}{2}\left(\frac{f}{\Gamma c}\right)^2 - \frac{ff'}{\Gamma c^2} - \frac{1}{Re}(cf')'\right]\mathrm{d}\eta + c_1(Z)$$

Here, c_1 is a function of z, which will be calculated by use of z momentum as

$$u\frac{\partial(\rho w)}{\partial r} + w\frac{\partial(\rho w)}{\partial z} = -\frac{\partial P}{\partial z}$$

But at

$$\begin{aligned}&r \to \infty\colon \rho w = 2Kz\rho_\infty \Rightarrow \begin{cases}\frac{\partial(\rho w)}{\partial r} = 0,\\ \frac{\partial(\rho w)}{\partial z} = 2K\rho_\infty\end{cases},\\ &\frac{\partial P}{\partial z} = \rho_\infty K^2 a^2\frac{\partial p}{\partial z}\end{aligned}$$

Then

$$\begin{aligned}&-\rho_\infty K^2 a^2\frac{\mathrm{d}c_1(z)}{\mathrm{d}z} = 2Kz(2K\rho_\infty) \Rightarrow \frac{\mathrm{d}c_1(z)}{\mathrm{d}z}\\ &\quad= -\frac{4z}{a^2} \Rightarrow c_1(z) = -2\left(\frac{z}{a}\right)^2\end{aligned}$$

which gives pressure as

$$p - p_0 = \int_0^\eta \left[\frac{1}{2}\left(\frac{f}{\Gamma c}\right)^2 - \frac{ff'}{\Gamma c^2} - \frac{1}{Re}(cf')'\right]\mathrm{d}\eta - 2\left(\frac{z}{a}\right)^2$$

To derive Eqs. (10) and (11), start from z momentum,

$$u\frac{\partial(\rho w)}{\partial r} + w\frac{\partial(\rho w)}{\partial z} = -\frac{\partial P}{\partial z} + \nu\left\{\frac{1}{r}\frac{\partial}{\partial r}\left[r\frac{\partial(\rho w)}{\partial r}\right] + \frac{\partial^2(\rho w)}{\partial z^2}\right\}$$

But

$$\begin{aligned}&\frac{\partial(\rho w)}{\partial r} = \frac{\partial(\rho w)}{\partial \eta}\frac{\partial \eta}{\partial r} = (2Kc'f'z + 2Kcf''z)\rho_\infty\frac{2r}{a^2}c \Rightarrow r\frac{\partial(\rho w)}{\partial r}\\ &\quad= (2Kcc'f'z + 2Kc^2f''z)\rho_\infty\frac{2r^2}{a^2} \Rightarrow \frac{\partial}{\partial r}\left[r\frac{\partial(\rho w)}{\partial r}\right]\\ &\quad= [2Kcc'f'z + 2Kc^2f''z]\rho_\infty\frac{4r}{a^2} + [2K(c')^2cf'z + 2Kc^2c''f'z\\ &\quad+ 6Kc^2c'f''z + 2Kc^3f'''z]\rho_\infty\frac{4r^3}{a^4} \Rightarrow \frac{1}{r}\frac{\partial}{\partial r}\left[r\frac{\partial(\rho w)}{\partial r}\right]\\ &\quad= [2Kcc'f'z + 2Kc^2f''z]\rho_\infty\frac{4}{a^2} + [2K(c')^2cf'z + 2Kc^2c''f'z\\ &\quad+ 6Kc^2c'f''z + 2Kc^3f'''z]\rho_\infty\frac{4}{a^2}\Gamma(\eta)\end{aligned}$$

Substitute in z momentum:

$$
\begin{aligned}
&-\frac{Ka^2}{r}\frac{\rho_\infty}{\rho}f(2Kc'f'z+2Kcf''z)\rho_\infty\frac{2r}{a^2}\frac{\rho}{\rho_\infty}\\
&+\frac{1}{\rho}(2K\rho_\infty cf'z)2K\rho_\infty\frac{\rho}{\rho_\infty}f'\\
&=\nu\Big\{[2Kcc'fz+2Kc^2f''z]\rho_\infty\frac{4}{a^2}+[2K(c')^2cf'z\\
&+2Kc^2c''f'z+6Kc^2c'f''z+2Kc^3f'''z]\rho_\infty\frac{4}{a^2}\Gamma(\eta)\Big\}\\
&-\rho_\infty K^2a^2\left(-\frac{4z}{a^2}\right)
\end{aligned}
$$

Equating the coefficient of z, the equation for f is

$$
\begin{aligned}
&-4K^2c'ff'-4K^2cff''+4K^2c(f')^2\\
&=\frac{8K\nu}{a^2}cc'f'+\frac{8K\nu}{a^2}c^2f''+\frac{8K\nu}{a^2}(c')^2c\Gamma f'+\frac{8K\nu}{a^2}c^2c''\Gamma f'\\
&+\frac{24K\nu}{a^2}c^2c'f''+\frac{8K\nu}{a^2}c^3\Gamma f'''+4K^2
\end{aligned}
$$

To derive the energy equation, Eq. (16), consider a change of variable as $T(\eta)/T_\infty = g(\eta)$. Then, the energy equation can be written as

$$\rho u\frac{\partial g}{\partial r}+\rho w\frac{\partial g}{\partial z}=\frac{\mu}{Pr}\frac{1}{r}\frac{\partial}{\partial r}\left(r\frac{\partial g}{\partial r}\right)$$

Using the chain rule,

$$
\begin{aligned}
&\frac{\partial g}{\partial r}=\frac{\partial g}{\partial\eta}\frac{\partial\eta}{\partial r}=\frac{2r}{a^2}cg', \qquad \frac{\partial g}{\partial z}=0\\
&r\frac{\partial g}{\partial r}=\frac{2r^2}{a^2}cg'\Rightarrow\frac{\partial}{\partial r}\left(r\frac{\partial g}{\partial r}\right)\\
&=\frac{4r}{a^2}cg'+(c'g'+cg'')\frac{4r^3}{a^4}c\Rightarrow\frac{1}{r}\left[\frac{\partial}{\partial r}\left(r\frac{\partial g}{\partial r}\right)\right]\\
&=\frac{4}{a^2}cg'+(c'g'+cg'')\frac{4r^2}{a^4}c\overset{r^2=a^2\Gamma(\eta)}{\rightarrow}\frac{1}{r}\left[\frac{\partial}{\partial r}\left(r\frac{\partial g}{\partial r}\right)\right]\\
&=\frac{4}{a^2}cg'+\frac{4\Gamma}{a^2}c(c'g'+cg'')
\end{aligned}
$$

By substitution,

$$-\frac{Ka^2}{r}\rho_\infty f\frac{2r}{a^2}\frac{\rho}{\rho_\infty}g'=\frac{\mu}{Pr}\frac{4}{a^2}(cg'+\Gamma cc'g'+\Gamma c^2g'')$$

Divide by $2k\rho$ and, because $1/Re = 2\nu/ka^2$,

$$\frac{1}{Re.Pr}(c^2\Gamma g''+\Gamma cc'g'+cg')+fg'=0$$

References

[1] Hiemenz, K., "Die Grenzschicht an einem in den gleichförmingen Flüssigkeitsstrom eingetauchten geraden Kreiszylinder," *Dinglers polytechnisches Journal*, Vol. 326, 1911, pp. 321–410.

[2] Homann, F. Z., "Der Einfluss Grosser Zahighkeit bei der Strmung um den Zylinder und um die Kugel," *Zeitschrift für angewandte Mathematik und Mechanik*, Vol. 16, 1936, pp. 153–164. doi:10.1002/zamm.19360160304

[3] Howarth, L., "The Boundary Layer in Three-Dimensional Flow. Part 2. The Flow Near Stagnation Point," *Philosophical Magazine*, Vol. 42, No. 7, 1951, pp. 1433–1440.

[4] Davey, A., "Boundary-Layer Flow at a Saddle Point of Attachment," *Journal of Fluid Mechanics*, Vol. 10, No. 4, 1961, pp. 593–610. doi:10.1017/S0022112061000391

[5] Wang, C. Y., "Axisymmetric Stagnation Flow on a Cylinder," *Quarterly of Applied Mathematics*, Vol. 32, 1974, pp. 207–213.

[6] Wang, C. Y., "Axisymmetric Stagnation Flow Towards a Moving Plate," *American Institute of Chemical Engineers Journal*, Vol. 19, No. 5, 1973, pp. 1080–1082. doi:10.1002/aic.690190540

[7] Gorla, R. S. R., "Heat Transfer in an Axisymmetric Stagnation Flow on a Cylinder," *Applied Scientific Research*, Vol. 32, No. 5, 1976, pp. 541–553. doi:10.1007/BF00385923

[8] Gorla, R. S. R., "Unsteady Laminar Axisymmetric Stagnation Flow over a Circular Cylinder," *Developments in Mechanics*, Vol. 9, 1977, pp. 286–288.

[9] Gorla, R. S. R., "Nonsimilar Axisymmetric Stagnation Flow on a Moving Cylinder," *International Journal of Engineering Science*, Vol. 16, No. 6, 1978, pp. 392–400.

[10] Gorla, R. S. R., "Transient Response Behavior of an Axisymmetric Stagnation Flow on a Circular Cylinder Due to Time-Dependent Free Stream Velocity," *Letters in applied and engineering sciences; an international Journal*, Vol. 16, No. 7, 1978, pp. 493–502. doi:10.1016/0020-7225(78)90082-4

[11] Gorla, R. S. R., "Unsteady Viscous Flow in the Vicinity of an Axisymmetric Stagnation-Point on a Cylinder," *International Journal of Engineering Science*, Vol. 17, No. 1, 1979, pp. 87–93. doi:10.1016/0020-7225(79)90009-0

[12] Cunning, G. M., Davis, A. M. J., and Weidman, P. D., "Radial Stagnation Flow on a Rotating Cylinder with Uniform Transpiration," *Journal of Engineering Mathematics*, Vol. 33, No. 2, 1998, pp. 113–128. doi:10.1023/A:1004243728777

[13] Grosch, C. E., and Salwen, H., "Oscillating Stagnation Point Flow," *Proceedings of Royal Society of London, Series A: Mathematical and Physical Sciences*, 384, No. 1786, 1982, pp. 175–190.

[14] Takhar, H. S., Chamkha, A. J., and Nath, J., "Unsteady Axisymmetric Stagnation-Point Flow of a Viscous Fluid on a Cylinder," *International Journal of Engineering Science*, Vol. 37, No. 15, 1999, pp. 1943–1957. doi:10.1016/S0020-7225(99)00009-9

[15] Saleh, R., and Rahimi, A. B., "Axisymmetric Stagnation-Point Flow and Heat Transfer of a Viscous Fluid on a Moving Cylinder with Time-Dependent Axial Velocity and Uniform Transpiration," *Journal of Fluids Engineering*, Vol. 126, No. 6, 2004, pp. 997–1005. doi:10.1115/1.1845556

[16] Rahimi, A. B., and Saleh, R., "Axisymmetric Stagnation-Point Flow and Heat Transfer of a Viscous Fluid on a Rotating Cylinder With Time-Dependent Angular Velocity and Uniform Transpiration," *Journal of Fluids Engineering*, Vol. 129, No. 1, 2007, pp. 107–115.

[17] Rahimi, A. B., and Saleh, R., "Similarity Solution of Unaxisymmetric Heat Transfer in Stagnation-Point Flow on a Cylinder with Simultaneous Axial and Rotational Movements," *Journal of Heat Transfer*, Vol. 130, No. 5, 2008, pp. 054502-1–054502-5.

[18] Abbasi, A. S., and Rahimi, A. B., "Non-Axisymmetric Three-Dimensional Stagnation-Point Flow and Heat Transfer on a Flat Plate," *Journal of Fluids Engineering*, Vol. 131, No. 7, 2009, pp. 074501.1–074501.5.

[19] Abbasi, A. S., and Rahimi, A. B., "Three-Dimensional Stagnation-Point Flow and Heat Transfer on a Flat Plate with Transpiration," *Journal of Thermophysics and Heat Transfer*, Vol. 23, No. 3, 2009, pp. 513–521. doi:10.2514/1.41529

[20] Abbasi, A. S., Rahimi, A. B., and Niazman, H., "Exact Solution of Three-Dimensional Unsteady Stagnation Flow on a Heated Plate," *Journal of Thermophysics and Heat Transfer*, Vol. 25, No. 1, 2011, pp. 55–58. doi:10.2514/1.48702

[21] Abbasi, A. S., and Rahimi, A. B., "Investigation of Two-Dimensional Stagnation-Point Flow and Heat Transfer Impinging on a Flat Plate," *Journal of Heat Transfer*, accepted as technical brief, 2011.

[22] Subhashini, S. V., and Nath, G., "Unsteady Compressible Flow in the Stagnation Region of Two-Dimensional and Axisymmetric Bodies," *Acta Mechanica*, Vol. 134, No. 3–4, 1999, pp. 135–145. doi:10.1007/BF01312652

[23] Kumari, M., and Nath, G., "Unsteady Compressible 3-Dimensional Boundary Layer Flow near an Axisymmetric Stagnation Point with Mass Transfer," *International Journal of Engineering Science*, Vol. 18, No. 12, 1980, pp. 1285–1300. doi:10.1016/0020-7225(80)90120-2

[24] Kumari, M., and Nath, G., "Self-Similar Solution of Unsteady Compressible Three-Dimensional Stagnation-Point Boundary Layers," *Journal of Applied Mathematics and Physics*, Vol. 32, No. 3, 1981.

[25] Katz, A., "Transformations of the Compressible Boundary Layer Equations," *SIAM Journal on Applied Mathematics*, Vol. 22, No. 4, 1972.

[26] Afzal, N., and Ahmad, S., "Effect of Suction and Injection on Self-Similar Solutions of Second-Order Boundary Layer Equations," *International Journal of Heat and Mass Transfer*, Vol. 18, No. 5, 1975, pp. 607–614. doi:10.1016/0017-9310(75)90272-0

[27] Libby, P. A., "Heat and Mass Transfer at a General Three-Dimensional Stagnation Point," *AIAA Journal*, Vol. 5, No. 3, 1967, pp. 507–517. doi:10.2514/3.4008

[28] Gersten, K., Papenfuss, H. D. and Gross, J. F., "Influence of the Prandtl Number on Second-Order Heat Transfer Due to Surface Curvature at a Three-Dimensional Stagnation Point," *International Journal of Heat and Mass Transfer*, Vol. 21, No. 3, 1978, pp. 275–284. doi:10.1016/0017-9310(78)90120-5

[29] Press, W. H., Flannery, B. P., Teukolsky, S. A., and Vetterling, W. T., *Numerical Recipes: The Art of Scientific Computing*, Cambridge Univ. Press, New York, 1997, p. 548.